



ELSEVIER

Available online at www.sciencedirect.com

SCIENCE @ DIRECT®

Physics of the Earth and Planetary Interiors 145 (2004) 19–36

PHYSICS
OF THE EARTH
AND PLANETARY
INTERIORS

www.elsevier.com/locate/pepi

Small-scale changes of core-mantle boundary reflectivity studied using core reflected PcP

Sebastian Rost*, Justin Revenaugh¹

Department of Earth Sciences, Center for the Study of Imaging and Dynamics of the Earth,
University of California Santa Cruz, 1156 High St., Santa Cruz, CA 95064, USA

Received 19 July 2003; accepted 5 February 2004

Abstract

Short-period PcP phases from earthquakes in the western Aleutians recorded at the Canadian Yellowknife array (YKA) sample the core-mantle boundary (CMB) beneath the Alaskan Kenai peninsula and the Cook inlet. The PcP -to- P amplitude ratios for these events show large variability with some amplitude ratios more than an order of magnitude larger than predicted by radial Earth models such as IASP91 or PREM. The amplitude ratios vary laterally with PcP core-mantle boundary reflection points showing a $\sim 1^\circ$ region with exceptionally large amplitude ratios. It is likely that the variability in relative PcP amplitudes is due in large part to CMB topography. Other mechanisms, such as radiation pattern; mantle attenuation; focusing and defocusing; and core-mantle boundary velocity and density perturbations could cause variations on scale-lengths of less than a degree as found in this study, but are unable to produce variations as large as those we observe.

© 2004 Elsevier B.V. All rights reserved.

Keywords: Core-mantle boundary; PcP ; Alaska; Reflection coefficient; Seismic array

1. Introduction

It has long been known that the core-mantle boundary (CMB) is a complicated compositional boundary within the Earth (Gutenberg, 1913) and characterized by strong lateral variations in physical properties and composition that extend upwards some ~ 300 km into the mantle (D'' , (Bullen, 1949)) (see Garnero,

2000, for a recent review). In recent years, strong heterogeneities in the lowermost mantle covering a wide scale-length range were discovered. The ~ 30 km zone surrounding the CMB is recognized as perhaps as heterogeneous and dynamic as the crust (see Garnero, 2000 for a review). The mantle-side structures atop the CMB are manifold, with scale-lengths from several thousands of kilometers (Garnero et al., 1998) to tens of kilometers (Rost and Revenaugh, 2003) and include, at a minimum, discontinuities (Lay and Helmberger, 1983; Weber and Davis, 1990; Thomas and Weber, 1997), anisotropy (Kendall and Silver, 1996) and thin layers with strongly reduced seismic velocities (ultra-low velocity zones, ULVZ) (Garnero and Helmberger, 1996; Revenaugh and Meyer, 1997; Garnero and Jeanloz, 2000; Rost and Revenaugh, 2003).

* Corresponding author. Tel.: +1-480-965-2413;

fax: +1-480-965-8102. Present address: Department of Geological Sciences, Arizona State University, Box 871404, Tempe, AZ 85287-1404, USA.

E-mail addresses: rstost@asu.edu (S. Rost), justinr@umn.edu (J. Revenaugh).

¹ Present address: Department of Geology and Geophysics, University of Minnesota, 310 Pillsbury Drive SE, Minneapolis, MN 55455, USA.

Core reflected phases like PcP and ScP provide direct localized pictures of the structures at the CMB and are well suited to resolving locally layered structures (Vidale and Benz, 1992; Garnero and Vidale, 1999). PcP is widely used to set constraints on the depth of the CMB (e.g. Jeffreys, 1939; Buchbinder and Poupinet, 1973; Engdahl and Johnson, 1974) and the radial changes of velocities and density across the CMB (e.g. Kanamori, 1967a). However, unexplained and substantial variations of the amplitude of short-period PcP preclude clear results and models of the CMB from PcP amplitudes normally include complicated transition zones from mantle to core (Buchbinder, 1965; Ibrahim, 1971a,b; Dubrovskiy and Pan'kov, 1972; Chowdury and Frasier, 1973; Buchbinder and Poupinet, 1973; Frasier and Chowdury, 1974; Schlittenhardt, 1986), whereas the CMB is described to be sharp and flat in radial Earth models like PREM (Dziewonski and Anderson, 1981) and IASP91 (Kennett and Engdahl, 1991). Some of these results are probably related to ULVZ, but even ULVZ cannot explain the range of amplitude variability (e.g. Castle and van der Hilst, 2000).

Some regions, in fact, show amplitudes that are as much as or more than an order of magnitude larger than predicted by radial Earth models (Tibuleac and Herrin, 1999; Castle and van der Hilst, 2000; Rost and Revenaugh, 2001).

We study P and PcP for earthquakes from the Aleutian subduction zone recorded at the Canadian Yellowknife array (YKA) (Manchee and Somers, 1966), sampling a region of the north-east Pacific nearby areas where previous studies find evidence for partial melt at the CMB (Revenaugh and Meyer, 1997), ULVZ for P -waves (Garnero and Helmberger, 1996) but not for S -waves (Castle and van der Hilst, 2000) and evidence for a sharp and flat CMB (Vidale and Benz, 1992; Persh et al., 2001). These studies suggest that this region of the CMB is complicated and will most likely show strong lateral variations.

Examining a region to the north-east of these studies, we observe PcP -to- P amplitude ratios with an amplification of more than an order of magnitude over theoretical ratios for radial Earth models like IASP91 (Kennett and Engdahl, 1991) or PREM (Dziewonski and Anderson, 1981) after correcting for source mechanism.

We discuss parameters other than structure at the CMB that affect the amplitude ratios and discuss different models of the CMB that might be able to increase the amplitude ratios over the $\lesssim 100$ km observed scale lengths.

2. Method

We compare both raw and source-corrected amplitudes of PcP to direct P (Fig. 1) giving us a measure of the P -wave reflection coefficient at the core-mantle boundary biased by propagation effects for both phases. Using (PcP/P) relative amplitudes minimizes crustal effects (Buchbinder, 1965) and eliminates the need for precise station gains, absolute moment information, etc. The same method was used previously to estimate the velocities and density around the CMB (Buchbinder, 1965; Dubrovskiy and Pan'kov, 1972; Chowdury and Frasier, 1973; Frasier and Chowdury, 1974). We use array data to increase the signal-to-noise ratio of small amplitude PcP phases and to determine the azimuthal direction of the incoming wave and its apparent velocity (slowness). Stacking of array records and using array averaged amplitude ratios from individual events also

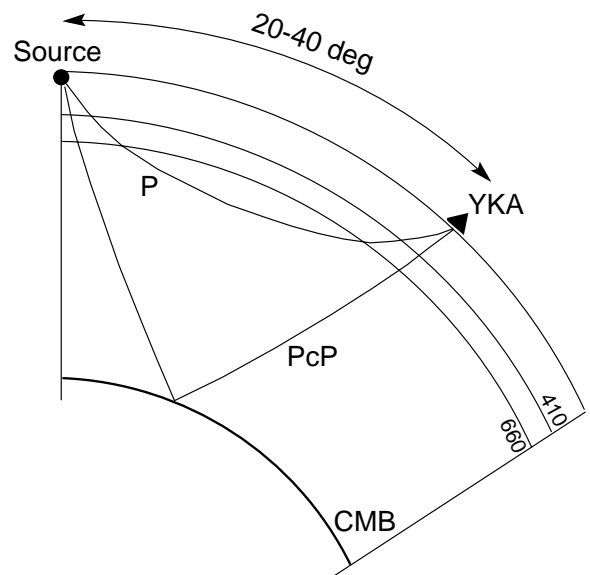


Fig. 1. Sketch of P and PcP raypaths. The epicentral distance between source and receiver for this study is between 20 and 40°.

decreases the influence of structures beneath the individual receivers. Due to the small size of the array, the take-off angles to the individual stations differ insignificantly and we interpret the mean array amplitudes for individual events rather than single-trace ratios. Large amplitude variations between closely spaced array stations have been described before (e.g. Tibuleac et al., 2003) and can also be found at YKA. Using averaged amplitude ratios reduces this problem. Nonetheless, the standard deviation of our averaged amplitude ratios is small, indicating small variation of the amplitudes at individual stations.

We measure peak-to-peak amplitudes in individual traces and compute the mean amplitude for the array from these individual values. We select events with a clearly identifiable *PcP* onset in the array recordings to avoid measuring average noise amplitudes in the *PcP* time window.

Due to the short epicentral distance sampled here (20–40°), the ray-paths of *PcP* and the direct *P*-wave differ substantially except very close to the source and the array. *PcP* travels through the attenuating upper mantle near vertically, whereas *P*, bottoming at 670–1000 km depth, spends a better part of its traveltimes in the uppermost mantle. *PcP*, on the other hand, travels a long path through the heterogeneous and perhaps strongly attenuating *D''* region of the lowermost mantle (Fisher et al., 2003). We take these differences into account when interpreting the amplitude ratios.

The take-off angles of *P* and *PcP* differ by about 20° for the distance range studied here. Therefore, the source excitations of the phases will differ, potentially quite substantially, so we correct raw observed (*PcP/P*) amplitude ratio using the full centroid moment tensor (CMT) solutions (e.g. Dziewonski et al., 1981). The radiation patterns for all events indicate that neither *PcP* nor *P* is within 15° of a nodal plane, but we acknowledge that the long-period CMT solutions are not optimal for our short-period observations. We conducted sensitivity tests by calculating synthetic seismograms while varying parameters of the CMT double-couple solution. These tests show that reasonable variation of the double-couple axes (strike, dip and slip) can account for a (*PcP/P*) amplitude ratio change of less than 20% if neither phase is close to a nodal plane.

3. Data

We use recordings of the Canadian Yellowknife array located in the northwestern territories. YKA is a small-aperture, short-period array of the United Kingdom Atomic Energy Administration type (Manchee and Somers, 1966), consisting of 18 vertical stations with a dominant frequency of about 1 Hz deployed along two perpendicular branches each ~20 km long.

Central Aleutian events from September 1989 to January 2002 recorded at YKA offer a unique opportunity to probe the CMB beneath Alaska (Fig. 2). From the YKA database we selected events with magnitudes larger than 5 with a range of depths from 0 to 275 km. We use the Engdahl et al. (1998) event relocations where available. For the most recent events, for which the Engdahl et al. (1998) relocations are unavailable, the source location information was obtained from the National Earthquake Information center. Selected earthquakes span longitudes from 170°E to 150°W. The final dataset consists of ~260 events with *PcP* identifiable in individual traces. The distance range extends from ~20 to ~40° with backazimuths θ from YKA of 267–306°. Most events are shallow with depths less than 50 km, but some events (22%) are deeper. Due to the high seismic activity of the Aleutian arc and the bow-shaped form of the seismicity, the *PcP* CMB reflection points form a compact and dense corridor beneath the Alaskan Kenai peninsula and the Cook inlet (see Fig. 2b). The proximity of the individual reflection points and use of high quality array data enables us to study the CMB in great detail.

In the 20–40° distance range, *PcP* arrives 4 1/2 to 2 min after *P* and outside the main body of the *P*-coda, which makes the identification of *PcP* easy, especially in array beam traces. The amplitude of *PcP* is usually $\lesssim 20\%$ of the *P* amplitude. Fig. 3a shows an example of much larger relative *PcP* amplitude (upper traces). The lower traces of Fig. 3a show synthetic seismograms calculated using the reflectivity method (Müller, 1985; Kind, 1985) including the Harvard CMT solution for this event, the IASP91 velocity model (Kennett and Engdahl, 1991) and the PREM (Dziewonski and Anderson, 1981) attenuation structure below 50 km. We employ a reflectivity algorithm that uses different source and receiver structure down to depths of 50–100 km (Kind, 1985) to account for the subduction related source region and the continental setting of

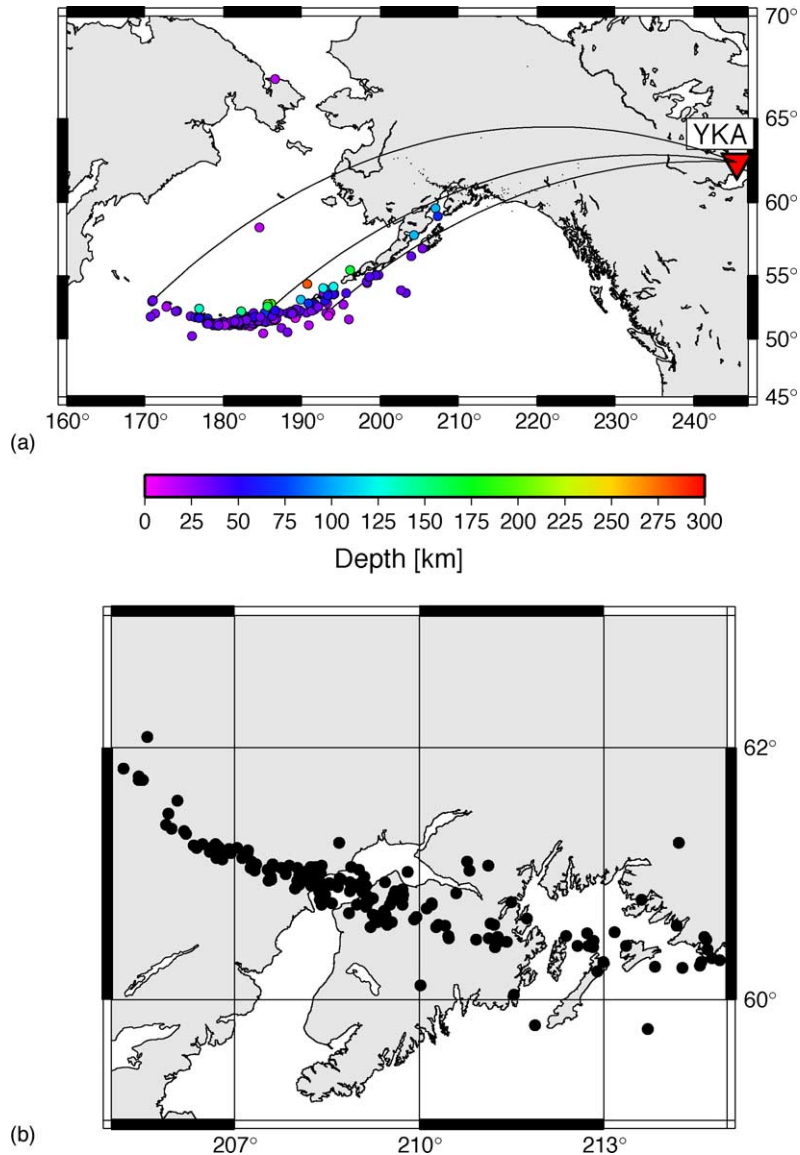
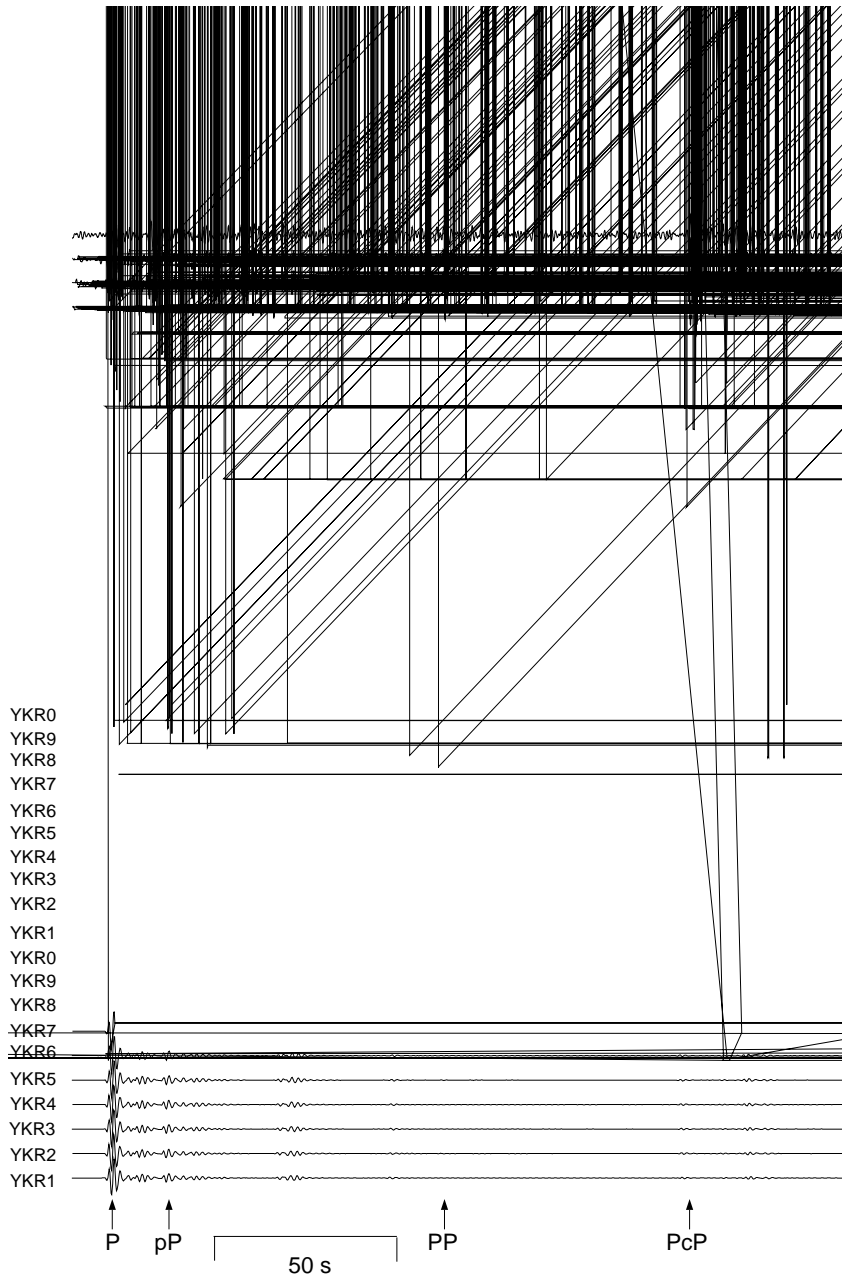


Fig. 2. (a) Map of event locations. We study central and eastern Aleutian events (circles) recorded at the small-aperture, short-period, vertical Yellowknife array (YKA) in northern Canada (triangle). Lines mark three examples for paths from source to receiver. Most of the events studied are shallow, but a few sources (22%) are located at depths of up to 300 km. (b) Map of PcP reflection points (circles) at the CMB, located beneath the Alaskan Kenai peninsula and the Cook inlet.

YKA. The reflectivity algorithm used here was tested against other codes that do not have the possibility to include different source and receiver structure. These test show that the amplitudes of P and PcP are correct in the method used here. We use the IASP91 velocity model and the PREM density structure, but change the

Q -model to account for the higher attenuation in the source region. All traces are aligned and normalized to the P -maximum. The differences between the synthetic traces and the data are striking. The first arrival and the depth phase pP are reasonably well fit (the PP arrival is underestimated due to the ambiguity between



source and receiver side structure for mid-path reflected phases in the numerical code used (Kind, 1985), which allows us to model structural differences on the source and receiver side), but the PcP amplitude in the synthetics is about 23% of P amplitude, whereas in data the ratio is $\sim 162\%$. Fig. 3b displays a different event, where the theoretical PcP amplitude is $\sim 4\%$ of P , but data is 154%. These examples show that some events in this region show PcP amplitudes that are more than an order of magnitude larger than predicted by one-dimensional (1D) Earth models.

4. Previous CMB studies beneath the north-west Pacific

Although the exact location of these CMB bounce points has not been probed for small-scale CMB structure before, a couple of studies have focussed on the CMB structure south-west of our study region. Vidale and Benz (1992) studied the CMB using both PcP and ScP phases from two Aleutian earthquakes recorded at stations in the Pacific north-west (US). They found the CMB to be flat and sharp, i.e. IASP91 like. A similar conclusion from a larger dataset was reached by Persh et al. (2001). With an even larger dataset, Castle and van der Hilst (2000) studied the same region to detect ultra-low shear velocities using ScP after the detection of ULVZ for P -waves in this region (Garnero and Helmberger, 1996). They also conclude that the CMB in this area is best modeled by an IASP91-like CMB for S -waves. Nonetheless, Castle and van der Hilst (2000) noticed unusually large ScP -to- P amplitude ratios, similar to those we observe for PcP , but they reached no conclusions about the source of these large amplitudes.

In agreement with this earlier study we detected some unusual large ScP amplitudes in our dataset. Nonetheless, the ScP -to- P amplitude ratios do not show values comparable to PcP -to- P nor do they show the small-scale variation we observe for PcP -to- P . Due to the different raypaths, ScP samples a different region of the CMB than the PcP waves used in this study. Several shear-wave studies find evidence for a variety of structures at the base of the mantle in the general Alaska region. These include shear-wave anisotropy (Garnero and Lay, 1997) and a $\sim 2.75\%$ shear-velocity increase ~ 240 – 280 km above the

CMB (Lay and Helmberger, 1983; Young and Lay, 1990).

5. PcP -to- P amplitude ratios

All measured PcP -to- P amplitude ratios are shown in Fig. 4. Fig. 4a shows the raw amplitude ratios (mean peak-to-peak array amplitude ratios for individual events) displayed at the PcP CMB reflection point. For 259 events we were able to identify PcP in the array recordings (nearly a magnitude more than previous studies, e.g. Frasier and Chowdury, 1974) with PcP reflection points in an area of only $\sim 10^\circ$ by 0.5° . Selection of clear PcP recordings introduces a slight bias towards larger PcP amplitudes, but avoids nodal arrivals that would be open to large amplitude uncertainties in synthetic calculations. All events also show strong P arrivals that are well above the noise level, which avoid unreasonable (PcP/P) amplitude ratios due to small or nodal P amplitudes.

The reflection points in the east and the west of the study area generally show amplitude ratios of less than 0.3 and are therefore only slightly larger than values predicted for IASP91. PcP -to- P amplitude ratios slightly larger than predicted by 1D Earth models are common in previous amplitude ratio studies (e.g. Frasier and Chowdury, 1974). In contrast, most events beneath the Cook inlet and the northwestern Kenai peninsula show much larger amplitude ratios—up to and often exceeding an order of a magnitude larger than predicted by IASP91 (see inserts of Fig. 4 for a clearer picture of the high amplitude ratio region).

Fig. 4b shows source normalized amplitude ratios. We calculate the theoretical radiation of PcP and P waves for each event using existing CMT solutions (e.g. Dziewonski et al., 1981). The full moment tensor is used to calculate the correction factors. The correction factors range between 0.14 and 8 (Fig. 5), but the vast majority of corrections are between 0.7 and 1.6. CMT solutions are available for 179 of the 259 events, accounting for the lower density of normalized events and biasing the survey towards larger events that were well enough recorded at teleseismic distances to determine a CMT solution. Unfortunately, no source mechanisms from regional distances for smaller earthquakes are published due to a lack of stations on the outer Aleutians [D. Christensen, per-

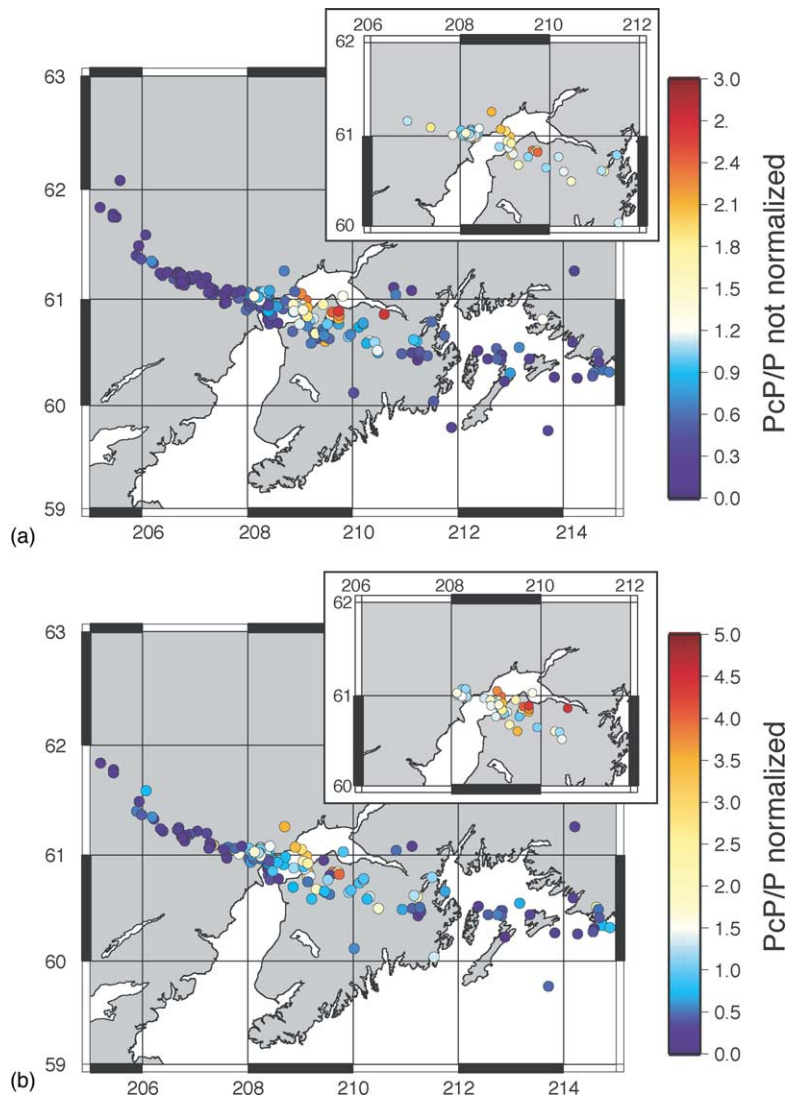


Fig. 4. (a) Map of the non-normalized PcP -to- P amplitude ratios. The amplitude ratios are plotted at the PcP reflection point at the CMB. Shown is the area beneath the Kenai peninsula and the Cook inlet. A small region shows very large amplitude ratios well above the expected values. The insert shows those amplitude ratios with values larger than 1.0 to focus on the high-amplitude-ratio region. (b) Same as (a) but showing normalized amplitude ratios. The amplitude ratios are normalized with the theoretical P and PcP amplitudes calculated from the CMT. More information is given in the text. The pattern in the amplitude ratios changes only slightly, but the high-amplitude region appears to be more compact than in the non-corrected case.

sonal communication, 2002; N. Ratchkovsh, personal communication, 2002]. The inclusion of the normalization does not change the broad picture of Fig. 4a, nonetheless, inclusion of the moment tensor correction factors reduces the scatter of the amplitude ratios slightly. The region beneath the Cook inlet still shows

high amplitude ratios, while the east and the west ends of the study area continue to show small amplitude ratios.

Due to the thin slice of seismicity along the Aleutian subduction zone we cannot observe the extension of the high amplitude ratios to the north. Nonetheless, we

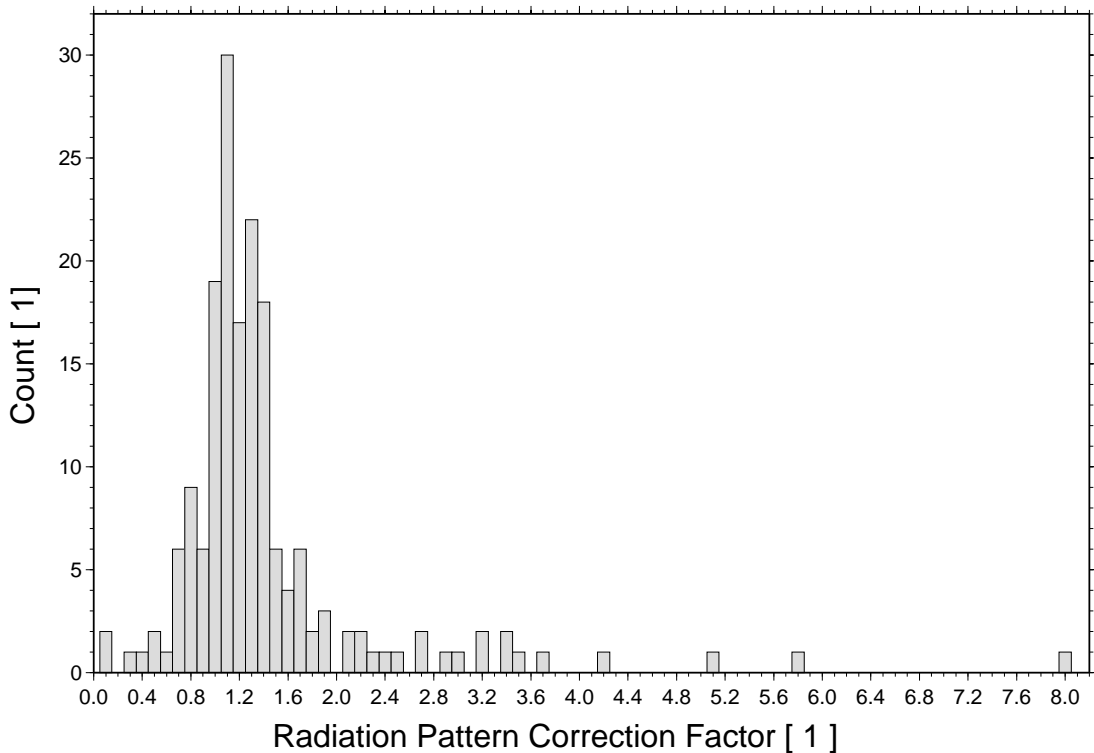


Fig. 5. Histogram of the applied source radiation normalization factor from CMT solutions. Most corrections are between 0.7 and 1.7, but a few events show very large corrections, an indication that one take-off angle is close to the nodal plane.

seem to capture the southern boundary of the anomalous region, since we observe nearly normal amplitude ratios to the south of the bright spot.

6. Discussion

A number of different mechanisms could contribute to the large *PcP*-to-*P* amplitude ratios we show in Fig. 4. Candidates include:

- (1) high attenuation along the *P*-path or low attenuation along the *PcP*-path;
- (2) focusing of *PcP* near the source, most likely in the subducting slab or defocusing of *P*, again most likely by the subducting slab;
- (3) systematic deviations of high-frequency radiation for compressional waves from the long-period moment tensors or lower quality estimate of the moment tensors in the region showing high amplitude ratios;

- (4) structure above the CMB, including changes in seismic velocities and density, and topography of the CMB;
- (5) structure immediately below the CMB.

The large amplitude ratios are not a pure distance effect as is shown in Fig. 6a. Most recordings are at distances between 32 and 36° and the amplitude ratio variation for these is large. Since the distances are so similar, geometric spreading can play only a minor role. We now discuss the possible contributions in detail.

6.1. Intrinsic attenuation

A strong change in *P*-wave attenuation of the mantle, either an increase of the quality factor *Q* along the *PcP* path or a decrease of *Q* along the *P* path, can increase the (*PcP*/*P*) amplitude ratio. The region of large ratios is about 1° in diameter (although the northern limit is not clear), i.e. 60–100 km depending

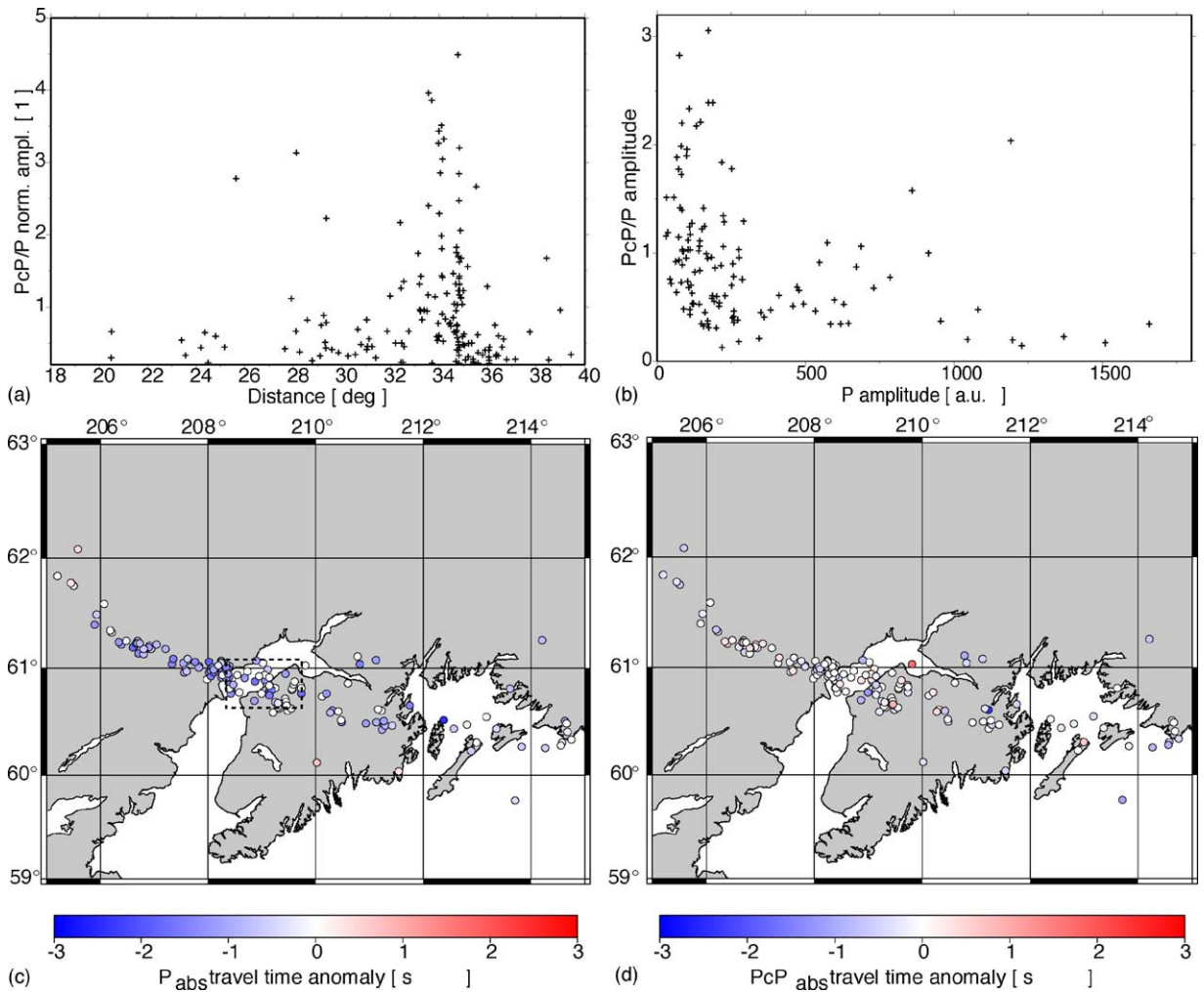


Fig. 6. (a) Distance dependent plot of amplitude ratios. The amplitude ratios exhibit much scatter and no trend with distance is discernible. We can exclude a pure distance dependent mechanism as the source of the high amplitude ratios. (b) PcP -to- P amplitude ratios vs. absolute P amplitudes (in arbitrary units). The amplitudes were measured in individual seismograms of YKA and then averaged for each event. The high amplitude ratios are not related solely to small P amplitudes. This excludes high attenuation of P in the upper mantle as the sole source of the high amplitude ratios. (c) Absolute P travel time anomaly shown at PcP CMB reflection points. The travel time anomaly was calculated relative to IASP91 travel times that are widely used for 1 Hz body waves. The region showing the high amplitude ratios is indicated by the dashed box. The high amplitude region is not marked by anomalous travel times, which is evidence that P does not sample high-attenuating and slow material in the upper mantle. (d) Same as (c) for PcP . No anomaly is visible in PcP that can be related to focusing of PcP in the high-velocity slab.

on the depth of the region. It is reasonable to assume that if strong attenuation of P , or very weak attenuation of PcP , is the reason for the high amplitude ratios, the region affecting the amplitudes is similar in size, i.e. about 100 km on a side. A region of this size is well below the resolution level of the tomographic at-

tenuation studies (Romanowicz, 1995; Bhattacharyya et al., 1996) and even below the resolution level of P -wave tomographic models (Kárason and van der Hilst, 1998). Tomographic models might indicate attenuating regions since attenuation is primarily due to thermal relaxation (e.g. Karato and Spetzler, 1990;

Káráson and van der Hilst, 2001) which is also connected to velocity variations.

Regional tomographic studies of the Pacific slab beneath Alaska (Engdahl and Gubbins, 1987; Kissling and Lahr, 1991) find evidence for a 80–100 km thick slab with a downdip length of 400 km and 4–11% higher velocity for P than the surrounding mantle. Since PcP leaves the slab area quickly, in-slab attenuation cannot explain the high PcP -to- P amplitude ratios. To produce the observed amplitude ratios by strong attenuation of P along a 100-km path requires a Q -factor of ≤ 10 . This is an extreme value that would require extensive partial melting at depths where P and PcP diverge significantly, i.e. ≥ 50 to 75 km depth. The regional tomographic models (Engdahl and Gubbins, 1987; Kissling and Lahr, 1991) do not show evidence for such a region. The alternative requires very large Q along the entire PcP path ($\sim 50,000$ given a reference value of 1000 for adjoining regions). Restricting the high Q region to a portion of the ray path increases this value tremendously. A study of attenuation structure from the Aleutian subduction zone to YKA (Sharrock et al., 1995) finds evidence for variation of attenuation along strike of the slab, but the variation is small and extreme values as are necessary to explain the amplitude ratio variations cannot be found.

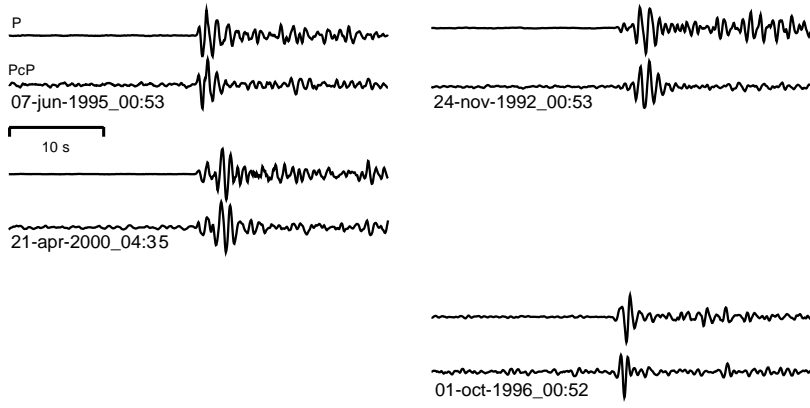
High attenuation along the P path is made more unlikely as the high amplitude ratios are not limited to small P amplitudes alone (Fig. 6b). Although several events show small P with PcP or small P amplitudes with large PcP amplitudes, we also observe large P amplitudes with even larger PcP amplitudes. In general, the largest amplitude ratios are observed for average P amplitudes paired large PcP amplitudes. High attenuation should also be visible in the P travel times due to the correlation of seismic velocities and attenuation (Karato and Spetzler, 1990), but we do not observe any trends in the absolute P -wave travel times (Fig. 6c) or in the absolute PcP travel times (Fig. 6d) that would indicate attenuation related to high temperature, i.e. slow seismic velocities. In Fig. 6c and d we show only travel time anomalies for events from 1989 to 1998, since for these events the high quality event relocations of Engdahl et al. (1998) exist, which show much smaller travel time anomalies. In general the travel time anomalies are relatively small, indicating that only minor inte-

grated velocity variations exist in the mantle in this region.

Lastly, if strong attenuation is the cause, the waveforms should reflect the frequency dependence of the attenuation. We do not observe any notable change in frequency content between the waveforms (Fig. 7) or in the spectra of the two phases. Note, that the similarity of these waveforms also indicates that PcP does not interact with ULVZ at the CMB and that most of this region of the CMB might be as sharp and simple as the well studied region a few degrees south-west of our study (Vidale and Benz, 1992; Castle and van der Hilst, 2000; Persh et al., 2001). In fact, we have only weak evidence for waveform variation due to ULVZ and no correlation with the high amplitude ratios can be made.

6.2. Slab focusing and multipathing

Both focusing of PcP in a low-velocity layer on top of the slab or multipathing and scattering of P in the slab influence the PcP -to- P amplitude ratios. Due to the source-receiver combination, P and PcP travel roughly along strike of the subducting slab. Kissling and Lahr (1991) resolve a thin, low-velocity layer on top of the high-velocity slab ($\Delta V_P \sim +5\%$) with P -wave velocity reductions of $\sim 10\%$. The influence of subduction zones on the wavefield has been studied before (Weber, 1990; Igel and Ita, 1997; Shapiro et al., 2000) but it has been found that focusing cannot produce amplitude variations on the short scale-lengths found here (Igel and Ita, 1997). More importantly, the paths for the high amplitude events leave the slab faster than events to the east due to the local slab configuration and we expect less influence from the slab for these western events. Also, if energy focusing in the fast slab occurs we would expect systematic travel time anomalies, evidence of which is not visible in Fig. 6d. The fast slab itself acts as an anti-waveguide defocussing the P -wave. Waveform studies of Aleutian events recorded in central Europe (Engdahl and Gubbins, 1987; Estabrook et al., 1997) (a path that travels perpendicular to the one used here) find strong P -wave coda energy related to the presence of oceanic crust in the source region. Nonetheless, Estabrook et al. (1997) do not find evidence for variation of coda energy along the slab, such that the variation in PcP -to- P amplitudes cannot be explained by scatter-



o

o variation of strike, dip and rake of the double

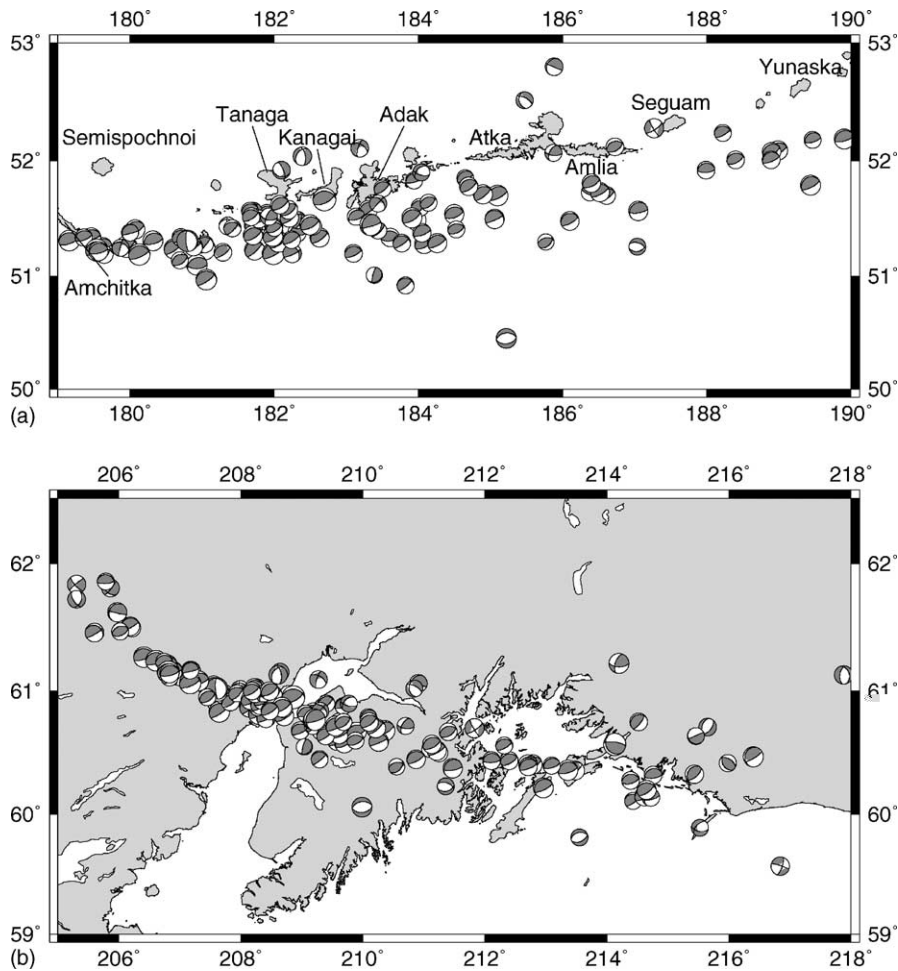


Fig. 8. (a) Published Aleutian CMT solutions (Dziewonski et al., 1981; Dziewonski and Woodhouse, 1983). Most events are thrust, which is in good agreement with the tectonic history of this region. The CMT solutions are very similar to the source mechanism determined using short-period data from the Adak network (Engdahl, 1971; LaForge and Engdahl, 1979; Engdahl and Billington, 1985; Engdahl and Kind, 1986). (b) Same as (a) but projected to the PcP CMB reflection points.

the amplitude ratios up to $\sim 20\%$; a substantial change but not nearly enough to explain our observations.

6.4. CMB velocity and density structure

PcP has been used to study material properties at the CMB for decades (e.g. Dana, 1945; Kanamori, 1967a,b; Ibrahim, 1971a,b; Dubrovskiy and Pan'kov, 1972; Frasier and Chowdury, 1974; Buchbinder and Poupinet, 1973; Chowdury and Frasier, 1973; Buchbinder, 1965) and large variations of PcP/P amplitude ratios have been found that are not explained

by radial Earth models. Seismic velocities and density in the mantle and the core control the P -wave reflection coefficient at the CMB, with varying influences. For the distance range of interest here, P -wave velocity reductions and density increases amplify the reflection coefficient, whereas it is decreased by a S -wave velocity reduction. For reasonable parameter changes associated with ULVZ, the reflection coefficient varies roughly proportionately (although sign varies). A 10% decrease in V_P raises the reflection coefficient $\sim 30\%$. A 10% increase in density lowers it by 10%. Lastly, a 30% decrease in V_S lowers the

coefficient by roughly a factor of 3. The net result is a lower reflection coefficient for models assuming coupled V_P and V_S reductions as is suggested by several studies (e.g. Williams and Garnero, 1996; Ni and Helmberger, 2001; Revenaugh and Meyer, 1997; Rost and Revenaugh, 2003).

The existence of a rigid layer at the top of the core (core-rigidity zone, CRZ) with a S -wave velocity of

~ 1 km/s, as detected between Tonga-Fiji and Australia (Rost and Revenaugh, 2003), would reduce the reflection coefficient by 24% and reduction of the core density due to, e.g. the conglomeration of “core sediments” (Braginsky, 1999; Buffett et al., 2000) would reduce the reflection coefficient further. All in all, it appears that the change of PcP due to ULVZ or CRZ is smaller than $\sim 50\%$ even for the most extreme

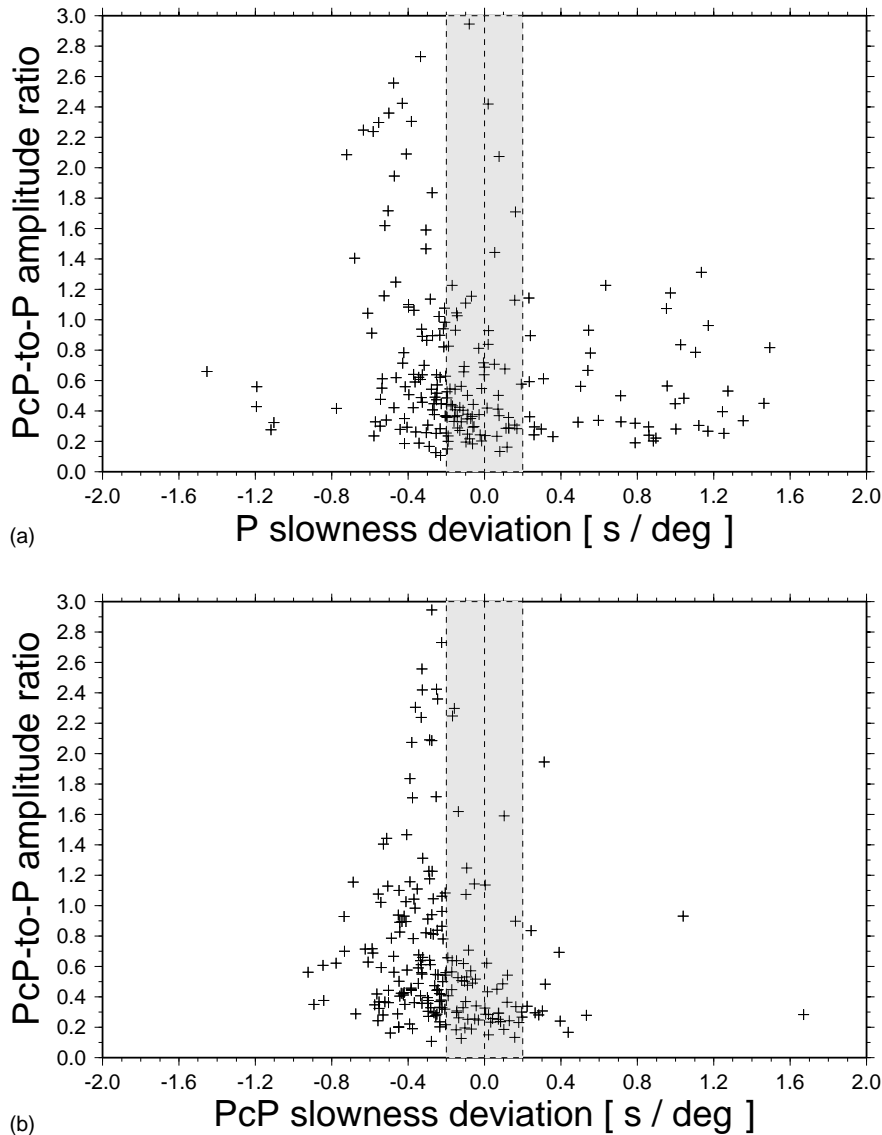


Fig. 9. (a) PcP -to- P amplitude ratios as function of the P slowness deviation from IASP91 values. We measure the slowness by fk -analysis. The shaded region gives the approximate slowness measurement error of the fk -analysis for YKA. (b) Same as (a) but for the PcP slowness deviation.

ULVZ and CRZ parameters and is opposite what is needed for more reasonable models, rendering such changes of seismic velocities and of density unable to explain an order-of-magnitude amplification of *PcP*. Even if they could, we do not observe the waveform complexities these structures must produce (e.g. Havens and Revenaugh, 2001; Rost and Revenaugh, 2003).

6.5. CMB topography

It is thought that topography on the CMB is responsible for some or much of the amplitude variation of *PcP* (e.g. Menke, 1986). Geodynamic modeling shows that CMB topography can be supported by small convection cells and topography with scale-lengths from the meter scale to hundreds of kilometers is

possible (e.g. Christensen, 1984; Narteau et al., 2001; Solomatov and Moresi, 2002). The influence of CMB topography on the seismic wavefield has been studied with physical (Menke, 1986) and synthetic models (Kampfmann and Müller, 1989; Neuberg and Wahr, 1991; Emmerich, 1993; Castle and van der Hilst, 2000). The studies by Kampfmann and Müller (1989) using *PcP* and Emmerich (1993) using *ScS* can be applied to our problem since both examine wavelengths scalable to the ones used here. They find that 2D “valley and ridge” topography with wavelengths of about 100 km, approximately the size of the Fresnel zone, introduces strong amplitude variations due to focusing and defocusing of the wavefield, while topography on wavelengths smaller than 50 km generates a general reduction of amplitudes without much variation, and longer wavelengths of topography

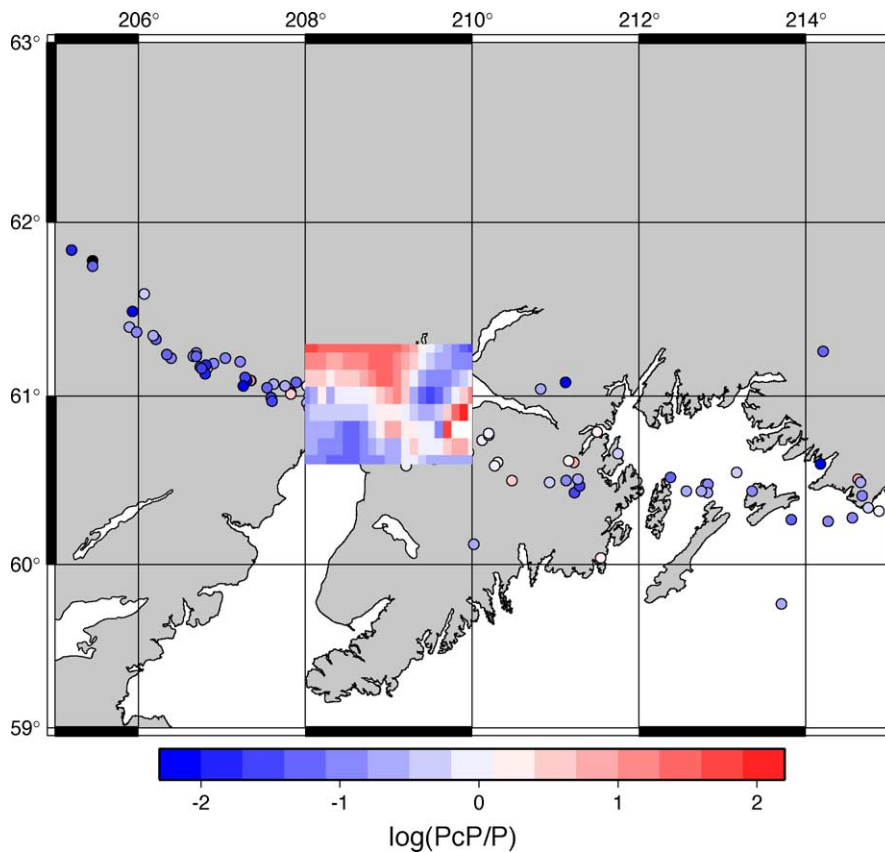


Fig. 10. Logarithmic amplitude ratios at location of *PcP* reflection point. The areas with high amplitudes and the highest density of reflection points is shown as surface to make trends in the data better observable.

introduce large amplitude variations but on scale-lengths larger than 10° . In any case, the analysis of *PcP* and *ScS* amplitudes (Kampfmann and Müller, 1989; Emmerich, 1993) suggests that reasonable 2D topography can only increase the *PcP* and *ScS* amplitudes by a factor of 2–3 and not by the order of magnitude we infer from our data. Castle and van der Hilst (2000) reach the same conclusion for *ScP* and considering reflections from a more complicated 3D “egg-crate” like topography. An increase of the CMB topography amplitude could increase the amplitude variation slightly (Kampfmann and Müller, 1989), but the maximum topography appears to be restricted to a few hundred meters in general (Doornbos, 1980; Vidale and Benz, 1992; Earle and Shearer, 1997, 1998), although smaller areas of greater relief are permitted, at least from the seismic data. Due to a lack of suitable 3D, 1 Hz wave propagation codes, we cannot study the possibility of topography as the cause of the amplitude variations in great detail.

We measured the slowness and backazimuth of *PcP* recorded at YKA. Fig. 9 shows the *PcP*-to-*P* amplitude ratio as function of the slowness deviation, the latter measured using fk-analysis (Aki and Richards, 1980; Capon, 1973) and relative to IASP91. The slowness resolution of YKA for these phases is approximately $0.2 \text{ s}/^\circ$. We detect slightly smaller than predicted slownesses for many events. Tabulated slowness-azimuth station corrections for YKA (Bondár et al., 1999) do not agree with the deviations found in our measurements, excluding the station underground as sole source for the found slowness deviations for *PcP* and *P*. Nonetheless, the slowness deviation is small and there is no apparent correlation between high amplitude ratios and slowness deviation. The small negative slowness deviation denotes a larger slowness in the data which indicates a shallower incident angle. Such a change would move the *PcP* reflection point $\sim 1.5^\circ$ towards the source and changes the *PcP* take-off angle a negligible 1° and results in a slightly asymmetric *PcP* path. This small slowness deviation might indicate a reflection off topography about 1.5° closer to the source that might be responsible for the high *PcP* amplitudes. But due to the similar *P* slowness deviation, the source of the deviation is most likely near the source.

We do not observe a systematic trend in the backazimuth measurements of *PcP* and *P*. This indicates

that both phases travel along great-circle paths, excluding a strong off-path focussing or defocussing at structures.

7. Conclusions

We present a dataset where very large changes in *PcP*-to-*P* amplitude ratios occur over short scale-lengths. We can exclude attenuation along the *PcP* and *P* paths and focusing effects in the upper mantle as the cause of the high amplitude ratios. Also, it is unlikely that the CMT solutions are systematically different from the short-period radiation pattern or the quality of the CMT's in and around the bright spot are of systematically lower quality.

We speculate that the most important mechanism for the high amplitude ratios is the CMB, although velocity structure alone cannot fully explain the amplification and the waveforms are in agreement with an IASP91-like CMB. This leaves topography of the CMB as the major cause of the high amplitude ratios, augmented by the other influences from the mechanisms discussed above. The lack of methods for calculating 1 Hz synthetic seismograms for small-scale structures at the CMB prevents a further study of the influence of the CMB topography on the *PcP* amplitudes. Fig. 10 shows a smoothed version of the logarithmic *PcP*-to-*P* amplitude ratios for the region with the highest density of *PcP* reflection points. There is evidence of a halo of reduced *PcP*-to-*P* ratios surrounding the high amplitude region. This is expected for the *PcP* focussing scenario, and backs the interpretation of high amplitude ratios as a focussing effect from structures at the CMB, although our data coverage does not allow a complete mapping of the focussing and defocussing zones.

In the end, the most important observation of this study is the apparent change of CMB reflectivity on very small scale-lengths. This is in agreement with other studies that find seismic evidence for small scale structure at the CMB (Havens and Revenaugh, 2001; Rost and Revenaugh, 2001, 2003).

Acknowledgements

We thank the Geological Survey of Canada and the CNSN datacenter for the YKA data. We thank Klaus

Stammler for his SeismicHandler software (Stammler, 1993). We thank Rainer Kind for making his reflectivity code available to us. Constructive reviews by John Castle and Paul Earle helped to improve this manuscript. Figures are produced using the GMT software by Wessel and Smith (1995). Funding for this study was provided by NSF grant EAR-9905733 and IGPP grant 02-GS-011. This is CSIDE contribution 477.

References

- Aki, K., Richards, P.G., 1980. *Quantitative Seismology, Theory and Methods*, vols. I and II. Freeman, San Francisco, 932 pp.
- Bhattacharyya, J., Masters, G., Shearer, P., 1996. Global lateral variations of shear wave attenuation in the upper mantle. *J. Geophys. Res.* 101, 22273–22289.
- Bondár, I., North, R.G., Beall, G., 1999. Teleseismic slowness-azimuth station corrections for the International Monitoring System seismic network. *Bull. Seism. Soc. Am.* 89, 989–1003.
- Braginsky, S.I., 1999. Dynamics of the stably stratified ocean at the top of the core. *Phys. Earth Planet. Int.* 111, 21–34.
- Buchbinder, G.G.R., 1965. *PcP* from the nuclear explosion BILBY, September 13, 1963. *Bull. Seism. Soc. Am.* 55, 441–463.
- Buchbinder, G.G.R., Poupinet, G., 1973. Problems related to *PcP* and the core-mantle boundary illustrated by two nuclear events. *Bull. Seism. Soc. Am.* 63, 2047–2070.
- Buffett, B.A., Garnero, E.J., Jeanloz, R., 2000. Sediments at the top of Earth's core. *Science* 290, 1338–1342.
- Bullen, K.E., 1949. Compressibility-pressure hypothesis and the Earth's interior. *Geophys. J. R. Astr. Soc.* 5, 355–368.
- Capon, J., 1973. Signal processing and frequency-wavenumber spectrum analysis for a large aperture seismic array. *Methods Comput. Phys.* 13, 1–59.
- Castle, J.C., van der Hilst, R.D., 2000. The core-mantle boundary under the Gulf of Alaska: no ULVZ for shear waves. *Earth Planet. Sci. Lett.* 176, 311–321.
- Chowdury, D.K., Frasier, C.W., 1973. Observation of *PcP* and *P* phases at LASA at distances from 26° to 40°. *J. Geophys. Res.* 78, 6021–6027.
- Christensen, U., 1984. Instability of a hot boundary layer and initiation of thermo-chemical plumes. *Ann. Geophys.* 2, 311–320.
- Dana, S.W., 1945. The amplitudes of seismic waves reflected and refracted at the Earth's core. *Bull. Seism. Soc. Am.* 35, 27–35.
- Doornbos, D.J., 1980. The effect of a rough core-mantle boundary on PKKP. *Phys. Earth Planet. Int.* 21, 351–358.
- Dubrovskiy, V.A., Pan'kov, V.L., 1972. On the amplitude ratio of the *PcP* and *P* waves. *Izv. Earth Phys.* 6, 81–83.
- Dziewonski, A.M., Chou, T.-A., Woodhouse, J.H., 1981. Determination of earthquake source parameters from waveform data for studies of global and regional seismicity. *J. Geophys. Res.* 86, 2825–2852.
- Dziewonski, A.M., Anderson, D.L., 1981. Preliminary reference Earth model. *Phys. Earth Planet. Int.* 25, 297–356.
- Dziewonski, A.M., Woodhouse, J.H., 1983. An experiment in systematic study of global seismicity; centroid-moment tensor solutions for 201 moderate and large earthquakes of 1981. *J. Geophys. Res.* 88, 3247–3271.
- Earle, P.S., Shearer, P.M., 1997. Observations of PKKP precursors used to estimate small-scale topography on the core-mantle boundary. *Science* 277, 667–670.
- Earle, P.S., Shearer, P.M., 1998. Observations of high-frequency scattered energy associated with the core phase PKKP. *Geophys. Res. Lett.* 25, 405–408.
- Ekström, G., Engdahl, E.R., 1989. Earthquake source parameters and stress distribution in the Adak island region of the central Aleutian islands, Alaska. *J. Geophys. Res.* 94, 15499–15519.
- Emmerich, H., 1993. Theoretical study on the influence of CMB topography on the core reflection *ScS*. *Phys. Earth Planet. Int.* 80, 125–134.
- Engdahl, E.R., 1971. Explosion effects and earthquakes in the Amchitka island region. *Science* 173, 1232–1235.
- Engdahl, E.R., Johnson, L.E., 1974. Differential *PcP* travel times and the radius of the core. *Geophys. J. R. Astr. Soc.* 39, 435–456.
- Engdahl, E.R., Billington, S., 1985. Focal depth determination of central Aleutian earthquakes. *Bull. Seism. Soc. Am.* 76, 77–95.
- Engdahl, E.R., Kind, R., 1986. Interpretation of broad-band seismograms from central Aleutian earthquakes. *Ann. Geophys.* B 4, 233–240.
- Engdahl, E.R., Gubbins, D., 1987. Simultaneous travel time inversion for earthquake location and subduction zone structure in the central Aleutian islands. *J. Geophys. Res.* 92, 13855–13862.
- Engdahl, E.R., van der Hilst, R.D., Buland, R.P., 1998. Global teleseismic earthquake relocation with improved travel times and procedures for depth determination. *Bull. Seism. Soc. Am.* 88, 722–743.
- Estabrook, C.H., Weber, M., Kind, R., 1997. Generation of the teleseismic *P*-wave coda from Aleutian earthquakes. *Geophys. J. Int.* 130, 349–364.
- Fisher, J.L., Wysession, M.E., Fischer, K.M., 2003. Small-scale lateral variations in *D''* attenuation and velocity structure. *Geophys. Res. Lett.* 30 (8), doi: 10.1029/2002GL016179.
- Frasier, C.W., Chowdury, D.K., 1974. Effect of scattering on *PcP/P* amplitude ratios at LASA from 40° to 84° distance. *J. Geophys. Res.* 79, 5469–5477.
- Garnero, E.J., 2000. Heterogeneity of the lowermost mantle. *Annu. Rev. Earth Planet. Sci.* 28, 509–537.
- Garnero, E.J., Jeanloz, R., 2000. Fuzzy patches on the Earth's core-mantle boundary? *Geophys. Res. Lett.* 27, 2777–2780.
- Garnero, E.J., Helmberger, D.V., 1996. Seismic detection of a thin lateral varying boundary layer at the base of the mantle beneath the central-Pacific. *Geophys. Res. Lett.* 23, 977–980.
- Garnero, E.J., Lay, T., 1997. Lateral variations in lowermost mantle shear wave anisotropy beneath the north Pacific and Alaska. *J. Geophys. Res.* 102, 8121–8135.
- Garnero, E.J., Revenaugh, J., Williams, Q., Lay, T., Kellogg, L.H., 1998. Ultralow velocity zones at the core-mantle boundary. In: M. Gurnis, M.E. Wysession, E. Knittle, B.A. Buffett (Eds.), *The Core-Mantle Boundary*. American Geophysical Union, Geodynamic Series, pp. 319–334.

- Garnero, E.J., Vidale, J.E., 1999. *ScP*; a probe of ultralow velocity zones at the base of the mantle. *Geophys. Res. Lett.* 26, 377–380.
- Gutenberg, B., 1913. Über die Konstitution des Erdinnern, erschlossen aus Erdbebenbeobachtungen. *Phys. Zeitschr.* 14, 1217–1218.
- Havens, E., Revenaugh, J., 2001. A broadband seismic study of the lowermost mantle beneath Mexico: constraints on ultralow velocity zone elasticity and density. *J. Geophys. Res.* 106, 30809–30820.
- Helmberger, D.V., Engen, G., Grand, S., 1985. Notes on wave propagation in laterally varying structure. *J. Geophys.* 58, 82–91.
- Ibrahim, A.K., 1971a. Effects of a rigid core on the reflection and transmission coefficients from a multi-layered core-mantle boundary. *Pure Appl. Geophys.* 91, 95–113.
- Ibrahim, A.K., 1971b. The amplitude ratio *PcP/P* and the core-mantle boundary. *Pure Appl. Geophys.* 91, 114–133.
- Igel, H., Ita, J., 1997. The effects of subduction zones on teleseismic SH waves: a numerical study. In: K. Fuchs (Ed.), *Upper Mantle Heterogeneities from Active and Passive Seismology*. Kluwer Academic Publishers, Dordrecht, pp. 333–341.
- Jeffreys, H., 1939. The times of *PcP* and *ScS*. *Month. Not. R. Astr. Soc.* 4, 537–547.
- Kampfmann, W., Müller, G., 1989. *PcP* amplitude calculations for a core-mantle boundary with topography. *Geophys. Res. Lett.* 16, 653–656.
- Kanamori, H., 1967a. Spectrum of *P* and *PcP* in relation to the mantle-core boundary and attenuation in the mantle. *J. Geophys. Res.* 72, 559–573.
- Kanamori, H., 1967b. Spectrum of short-period core phases in relation to the attenuation in the mantle. *J. Geophys. Res.* 72, 2181–2187.
- Karato, S., Spetzler, H.A., 1990. Defect microdynamics in minerals and solid-state mechanisms of seismic wave attenuation and velocity dispersion in the mantle. *Rev. Geophys.* 28, 399–421.
- Káráson, H., van der Hilst, R.D., 1998. An improved model for whole mantle *P*-wavespeed based on travel time data of *P*, *pP*, *PP*, *PKP* and *P_{diff}* phases. *EOS Trans. Suppl.* 79, 220.
- Káráson, H., van der Hilst, R.D., 2001. Tomographic imaging of the lowermost mantle with differential times of refracted and diffracted core phases (*PKP*, *P_{diff}*). *J. Geophys. Res.* 106, 6569–6587.
- Kennett, B.L.N., Engdahl, E.R., 1991. Traveltimes for global earthquake location and phase identification. *Geophys. J. Int.* 105, 429–465.
- Kendall, J.-M., Silver, P.G., 1996. Constraints from seismic anisotropy on the nature of the lowermost mantle. *Nature* 381, 409–412.
- Kind, R., 1985. The reflectivity method for different source and receiver structures and comparison with GRF data. *J. Geophysics* 58, 146–152.
- Kissling, E., Lahr, J.C., 1991. Tomographic image of the Pacific slab under southern Alaska. *Eclogae geol. Helv.* 84, 297–315.
- LaForge, R., Engdahl, E.R., 1979. Tectonic implications of seismicity in the Adak canyon region, central Aleutians. *Bull. Seism. Soc. Am.* 69, 1515–1532.
- Lay, T., Helmberger, D.V., 1983. A lower mantle *S*-wave triplication and the shear velocity structure of *D''*. *Geophys. J. R. Astr. Soc.* 75, 799–837.
- Manchee, E., Somers, H., 1966. The Yellowknife seismological array. *Publ. Dominion Observ. Ottawa* 32, 69–84.
- Menke, W., 1986. Few 2–50 km corrugations on the core-mantle boundary. *Geophys. Res. Lett.* 13, 1501–1504.
- Müller, G., 1985. The reflectivity method: a tutorial. *J. Geophys.* 58, 153–174.
- Nataf, H.-C., VanDecar, J., 1993. Seismological detection of a mantle plume? *Nature* 364, 115–120.
- Narteau, C., LeMouél, J.L., Poirier, J.P., Sepúlveda, E., Shnirman, M., 2001. On a small-scale roughness of the core-mantle boundary. *Earth Planet. Sci. Lett.* 191, 49–60.
- Neuberg, J., Wahr, J., 1991. Detailed investigation of a spot on the core-mantle boundary using digital *PcP* data. *Phys. Earth Planet. Int.* 68, 132–143.
- Ni, S., Helmberger, D.V., 2001. Probing an ultra-low velocity zone at the core mantle boundary with *P* and *S* waves. *Geophys. Res. Lett.* 28, 2345–2348.
- Persh, S.E., Vidale, J.E., Earle, P.S., 2001. Absence of short-period ULVZ precursors to *PcP* and *ScP* from two regions of the CMB. *Geophys. Res. Lett.* 28, 387–390.
- Revenaugh, J., Meyer, R., 1997. Seismic evidence of partial melt within a possibly ubiquitous low-velocity layer at the base of the mantle. *Science* 277, 670–673.
- Ritsema, J., van-Heijst, H.-J., Woodhouse, J.H., 1999. Complex shear wave velocity structure imaged beneath Africa and Iceland. *Science* 286, 1925–1928.
- Romanowicz, B., 1995. A global tomographic model of shear attenuation in the upper mantle. *J. Geophys. Res.* 100, 12375–12394.
- Rost, S., Revenaugh, J., 2001. Seismic detection of rigid zones at the top of the core. *Science* 294, 1911–1914.
- Rost, S., Revenaugh, J., 2003. Small-scale ultra-low velocity zone structure imaged by *ScP*. *J. Geophys. Res.* 108 (B1), doi: 10.1029/2001JB001627.
- Schlittenhardt, J., 1986. Investigation of the velocity- and *Q*-structure of the lowermost mantle using *PcP/P* amplitude ratios from arrays at distances of 70°–84°. *J. Geophys.* 60, 1–18.
- Shapiro, N.M., Olsen, K.B., Singh, S.K., 2000. Wave-guide effects in subduction zones: evidence from three-dimensional modeling. *Geoph. Res. Lett.* 27, 433–436.
- Sharrock, D.S., Main, I.G., Douglas, A., 1995. Observations of *Q* from the northwest Pacific subduction zone recorded at teleseismic distances. *Bull. Seism. Soc. Am.* 85, 237–252.
- Solomatov, V.S., Moresi, L.N., 2002. Small-scale convection in the *D''* layer. *J. Geophys. Res.* 107 (B1), doi: 10.1029/2000JB000063.
- Stammler, K., 1993. SeismicHandler; programmable multichannel data handler for interactive and automatic processing of seismological analyses. *Comput. Geosci.* 19, 135–140.
- Thomas, C., Weber, M., 1997. *P* velocity heterogeneities in the lower mantle determined with the German Regional Seismic Network: improvement of previous models and results of 2D modelling. *Phys. Earth Planet. Int.* 101, 105–117.

- Tibuleac, I.M., Herrin, E., 1999. Lower mantle lateral heterogeneity beneath the Caribbean sea. *Science* 285, 1711–1715.
- Tibuleac, I.M., Nolet, G., Caryl, M., Koulakov, I., 2003. *P* wave amplitudes in a 3D earth. *Geophys. J. Int.* 155, 1–10.
- Vidale, J.E., Benz, H.M., 1992. A sharp and flat section of the core-mantle boundary. *Nature* 359, 627–629.
- Weber, M., 1988. Computation of body-wave seismograms in absorbing 2D media using the Gaussian beam method: comparison with exact methods. *Geophys. J. Int.* 92, 9–24.
- Weber, M., 1990. Subduction zones—their influence on traveltimes and amplitudes of *P*-waves. *Geophys. J. Int.* 101, 529–544.
- Weber, M., Davis, J.P., 1990. Evidence of a laterally variable lower mantle structure from *P*- and *S*-waves. *Geophys. J. Int.* 102, 231–255.
- Wessel, P., Smith, W.H.F., 1995. New version of the generic mapping tools released. *Trans. Am. Geophys. Union (EOS)* 76, 329.
- Williams, Q., Garnero, E.J., 1996. Seismic evidence for partial melt at the base of Earth's mantle. *Science* 273, 1528–1530.
- Young, C.J., Lay, T., 1990. Multiple phase analysis of the shear velocity structure in the *D'* region beneath Alaska. *J. Geophys. Res.* 95, 17385–17402.
- Zhao, D., Christensen, D., Pulpan, H., 1995. Tomographic imaging of the Alaskan subduction zone. *J. Geophys. Res.* 100, 6487–6504.
- Zhao, D., 2001. Seismic structure and origin of hotspots and mantle plumes. *Earth Planet. Sci. Lett.* 192, 251–265.